Isotopic Evolution of Mauna Loa Volcano: A View From the Submarine Southwest Rift Zone

Mark D. Kurz, T. C. Kenna, D. P. Kammer

Department of Marine Chemistry and Geochemistry, Woods Hole Oceanographic Institution, Woods Hole, MA

J. Michael Rhodes

University of Massachusetts, Amherst, MA

Michael O. Garcia

University of Hawaii, Honolulu, HI

New isotopic and trace element measurements on lavas from the submarine southwest rift zone (SWR) of Mauna Loa continue the temporal trends of subaerial Mauna Loa flows, extending the known compositional range for this volcano, and suggesting that many of the SWR lavas are older than any exposed on land. He and Nd isotopic compositions are similar to those in the oldest subaerial Mauna Loa lavas (Kahuku and Ninole Basalts), while $^{87}Sr/^{86}Sr$ ratios are slightly lower (as low as .7036) and Pb isotopes are higher ($^{206}Pb/^{204}Pb$ up to 18.30). The coherence of all the isotopes suggests that helium behaves as an incompatible element, and that helium isotopic variations in the Hawaiian lavas are produced by melting and mantle processes, rather than magma chamber or metasomatic processes unique to the gaseous elements. The variations of He, Sr, and Nd are most pronounced in lavas of approximately 10 ka age range [*Kurz and Kammer*, 1991], but the largest Pb isotopic variation occurs earlier. These variations are interpreted as resulting from the diminishing contribution from the upwelling mantle plume material as the shield building ends at Mauna Loa. The order of reduction in the plume isotopic signature is inferred to be Pb (at >100 ka), He (at ~14 ka), Sr (at ~9 ka), and Nd (at ~8 ka); the different timing may relate to silicate/melt partition coefficients, with most incompatible elements removed first, and also to concentration variations within the plume. Zr/Nb, Sr/Nb, and fractionation-corrected Nb concentrations, correlate with the isotopes and are significantly higher in some of the submarine SWR lavas, suggesting temporal variability on time scales similar to the Pb isotopes (i.e. ~ 100 ka). Historical lavas define trace element and isotopic trends that are distinct from the longer term (10 to 100 ka) variations, suggesting that different processes cause the short term variability. The temporal evolution of Mauna Loa, and particularly the new data from the submarine SWR, suggest that the isotopic composition of the upwelling plume mantle is best represented by data from Loihi seamount tholeiites. The temporal evolution suggests that the mantle source of the latest stage of Mauna Loa, which is characterized by radiogenic $^{87}Sr/^{86}Sr$ (up to .70395), unradiogenic $^{206}Pb/^{204}Pb$ (~18.0), $^{3}He/^{4}He$ ratios similar to MORB, and low Nb concentrations, is a small-volume contribution related to non-plume components (such as normal asthenosphere, or entrained mantle).

Mauna Loa Revealed: Structure,
Composition, History, and Hazards
Geophysical Monograph 92

1. INTRODUCTION

Previous studies of Mauna Loa volcano have shown that isotopic compositions of lava flows have significantly

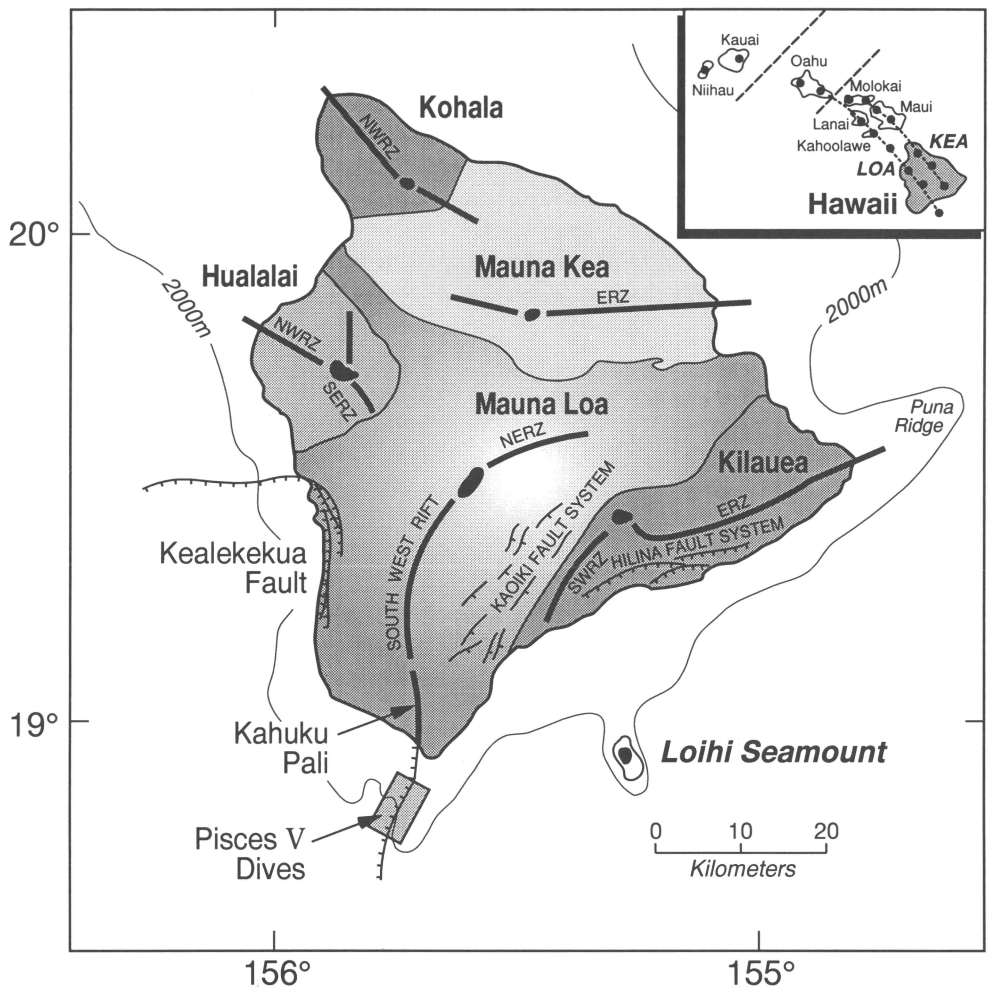

Figure 1. Map of Hawaii showing the principal rift zones of the Hawaiian volcanoes, and the study area on the submarine southwest rift zone (SWR) sampled during Pisces V dives 182-185 [see also *Garcia et al.*, this volume]. Dark areas are the volcano summits.

changed on eruptive time scales between 0.1 and 10 ka [*Kurz et al.*, 1987; *Kurz and Kammer*, 1991; *Kurz*, 1993]. A marked decrease in $^{3}He/^{4}He$ at approximately 10 ka, suggests a diminished hotspot influence beneath Mauna Loa, in accord with a decline in eruption rates since about 100 Ka inferred from geologic data [e.g. *Lipman et al.*, 1990; *Moore et al.*, 1990; *Lipman*, this volume]. If the hotspot supply to Mauna Loa diminished since 10 ka, as implied by the helium data, then this volcano offers a special opportunity to study a critical transition of Hawaiian volcano evolution.

Mauna Loa is an ideal place to study temporal evolution of volcanism because of its frequent historical eruptions and the excellent stratigraphic framework provided by geologic mapping combined with radiocarbon dating [e.g., *Lipman and Swenson*, 1984; *Lockwood and Lipman*, 1987; *Rubin et al.*, 1987; *Lockwood*, 1995]. The oldest stratigraphically exposed Mauna Loa lavas are along the Kahuku and Kealekekua faults and in the Ninole Hills (see Figure 1). This paper presents new isotopic and trace element data from the submarine southwest rift zone of Mauna Loa (SWR), on the Kahuku fault, which extend the age range of analyzed lavas and provide insights into the causes of the geochemical variations. We also present additional trace element and Nd isotopic data for the samples discussed by *Kurz and Kammer* [1991], which demonstrate coherent variations among the trace elements and the Sr, Nd, Pb, and He isotopic systems.

The isotopic variations among Mauna Loa lavas are important to global geochemical models because such detailed stratigraphic sequences are available for few oceanic islands. Coherent variations in the isotopes of He, Sr, and Pb rule out many of the models that have been invoked to "decouple" helium from the radiogenic isotopes, such as

metasomatism, magma chamber degassing, and radiogenic ingrowth of ^{4}He [e.g. *Condomines et al.*, 1983; *Zindler and Hart*, 1986; *Vance et al.*, 1989; *Hilton et al.*, 1995]. However, the complexity of the Mauna Loa isotopic variations may require the presence of three distinct mantle sources, combined with plate movement and waning of the hotspot [*Kurz and Kammer*, 1991]. The oldest Mauna Loa lavas have the highest ^{3}He/^{4}He ratios, while the historical lavas have low ^{3}He/^{4}He ratios similar to normal mid-ocean ridge basalts (MORB). The high ^{3}He/^{4}He ratios identify the source of the oldest Mauna Loa shield lavas as the upwelling mantle plume, and the other two sources may relate either to lithosphere, normal asthenosphere, or entrained asthenosphere [*Kurz and Kammer*, 1991; *Kurz*, 1993]. An alternative explanation is that the complex isotopic variations are produced by only two mantle sources (plume and normal asthenosphere), coupled with the effects of melt percolation through a porous medium and chromatographic separation of different elements [*McKenzie and O'Nions*, 1991; *Watson*, 1993]. Determining the geometry of mantle heterogeneities and melting processes remains one of the difficulties of reconciling geochemical and geophysical observations. The explanation for the short-timescale Mauna Loa isotopic variations is important not just for understanding the present-day configuration of the largest volcano on earth, but to the processes of melting in the mantle.

2. SAMPLES AND ANALYTICAL METHODS

2.1. *Samples*

The ^{14}C age and Sr, Nd, Pb and He isotopic data for subaerial Mauna Loa lavas are presented in table 1 (radiocarbon dated and historical) and table 2 (Kahuku and Ninole); sample localities have been discussed elsewhere [*Kurz et al*, 1983; *Kurz et al.*, 1987; *Kurz and Kammer*, 1991]. The samples in tables 1 and 2 are assigned a stratigraphic order, as reflected in "unit number" which increases with age. For the Kahuku samples, stratigraphic order is simply related to depth in section on the Kahuku Pali; the samples range from the youngest (top of the section) to the oldest. The top of the Kahuku Pali is covered with Pahala ash, which is generally assumed to be older than 31 ka [*Lipman and Swenson*, 1984; *Lockwood and Lipman*, 1987]. Unit numbers 17 and 18 directly underlie the Pahala ash and occur at the top of the Kahuku fault, and are assumed to be >31 ka in age. Unit number 19 is from the base of the Kealekekua fault [*Kurz and Kammer*, 1991], placing it below the Pahala ash (and hence older than units 17 and 18); the placement of this unit with respect to the other Kahuku exposures is speculative, but it is assumed here to be younger. Ninole Basalt, exposed on the southern flank of Mauna Loa, has been dated at 100 to 200 ka in age [*Lipman et al.*, 1990], and is assumed to be older than the subaerial Kahuku Basalts. Data for most of the Kahuku and Ninole lavas and their relative locations are given in *Kurz and Kammer* [1991]. The only new subaerial Mauna Loa samples in the tables are KS87-26 and KS87-27 (table 2), which were collected from 41 and 38 meters (above sea level) on the Kahuku fault, at the same location described in *Kurz and Kammer* [1991].

Pisces V dives 182-185 were carried out on the submarine portion of the Kahuku fault (see Figure 1) between 550 and 2000 meters below sea level [*Garcia et al.*, this volume]. A primary objective was to extend the stratigraphy back in time, which is possible because there has been little recent activity on the submarine portion of the Kahuku fault, and the exposed sections are not covered by recent lavas [*Fornari et al.*, 1979; *Moore et al.*, 1990; *Moore and Clague*, 1992; *Garcia et al.*, this volume]. *Lipman* [this volume] discusses attempts to K-Ar date these lavas, which have been unsuccessful due to the young ages, low K contents, and excess (mantle) ^{40}Ar. The subsidence rate for Hawaii of 2.5 mm/yr [*Moore*, 1987] and the depth would imply ages between 200 and 800 ka. However, because all of the flows have glassy, pillow morphology, it is certain that they were erupted under water, and the subsidence rates provide only upper age limits. Based on subsidence rates for a submerged shoreline on the SWR, *Lipman* [this volume] suggests a minimum age of 130-150 ka for the top of the submarine section. In summary, age estimates for the submarine Southwest rift lavas are 100-300 ka, but must be viewed as tentative [*Garcia et al.*, this volume; *Lipman*, this volume].

The dive samples from the SWR are considered to be a continuation of the subaerial Kahuku section, which represents a fault or landslide scar [*Garcia et al.*, this volume]. Although the age constraints do not exclude the possibility that there is age overlap between the subaerial and submarine samples, the dive samples represent an age sequence on a single stratigraphic section. Samples collected during dives 182 and 183 are a continuous depth (and hence stratigraphic) traverse of this sequence at one location. The two samples from dive 185 were collected from the top of the fault, and are assumed to be the youngest samples, even though they were collected from 1400 to 1700 meters water depth. The samples from dive 184 are placed relative to the others based on the reconstructed section presented by *Garcia et al.* [this volume]. As discussed below, the isotopic data, presented in table 3, suggest that at least some of the submarine SWR lavas are older than the subaerial Kahuku and Ninole Basalts, and therefore are consistent with ages greater than 100-200 ka. Further dis-

TABLE 1. Isotopic and Trace Element Data for Historical and Radiocarbon Dated Lava Flows

sample	ML55(1950)	ML82(1887)	185	187	202	ML84(1868)	k7-03#	k7-05	K7-15	k7-31#	ha82-01#
Unit #	1	2	3	3	3	4	5	5	5	6	7
age(yrs)*	0	63	73	73	73	82	640	640		890	910
$^3He/^4He$	8.6	8.6	8.2	8.2	8.3	8.0	8.5	8.6		8.8	8.1
±	0.4	0.2	0.2	0.2	0.2	0.8	0.1	0.1		0.3	0.1
$^{87}Sr/^{86}Sr$	0.703826	0.703857	0.703857	0.703825	0.703857	0.703853	0.703930	0.703936	0.703942	0.703957	0.703950
$^{206}Pb/^{204}Pb$	18.11	18.16	18.13	18.11	18.14	18.14		18.08		18.10	18.09
$^{207}Pb/^{204}Pb$	15.46	15.44	15.44	15.43	15.45	15.45		15.45		15.44	15.46
$^{208}Pb/^{204}Pb$	37.91	37.88	37.85	37.82	37.88	37.88		37.85		37.85	37.87
$^{143}Nd/^{144}Nd$	0.5128945	0.512894		0.5128843	0.512903	0.5128775	0.5128327	0.512838	0.5128373	0.512827	0.5128373
MgO	8.65	8.53				22.21	15.54			8.28	15.42
Sr/Y	13.5	12.3				14.3	13.7			13.3	12.1
K/Y	133.4	122.7				145.7	160.9			154.2	156.8
Sr/Nb	31.8	30.9				32.0	26.9			29.3	26.9
K/Sr	9.9	10.0				10.2	11.7			11.6	12.9
Zr/Nb	13.2	13.5				13.1	12.3			13.2	13.4
Zr/Y	5.6	5.4				5.9	6.3			6.0	6.0
K/P							2.6			2.8	2.8
Rb	5.2	5.0				4.2	5.9			7.4	6.5
Sr	296	275				205	266			345	272
Nb	9.3	8.9				6.4	9.9			11.8	10.1
Zr	123	120				84	122			156	135
Y	21.9	22.4				14.3	19.4			26.0	22.4

cussion of the field relations, geological context, and petrology of these samples is presented by *Garcia et al.* [this volume] and *Lipman* [this volume] in this volume.

2.2. *Analytical Methods*

Analytical methods for the measurement of Sr, Pb, and He have been presented elsewhere [*Kurz et al.*, 1987; *Kurz and Kammer,* 1991]. The Nd isotopic measurements were carried out on aliquots of the same whole rock sample previously used for the Sr and Pb measurements. The Nd chemistry was carried out on either the unused fraction from the Pb chemistry, or separate dissolutions, using the methylactic acid technique. The Nd was loaded onto the Ta side filament of Ta-Re double filament, and the isotopes measured on a VG 354 thermal ionization mass spectrometer using dynamic multicollection. The $^{143}Nd/^{144}Nd$ ratios are fractionation-corrected using a $^{146}Nd/^{144}Nd$ ratio of .7219, and normalized to a La Jolla value of .51184. During the course of this study, the average measured value for the La Jolla standard was .511851 (± .000008, n=25). Typical statistics on an individual sample run are 10 ppm on $^{143}Nd/^{144}Nd$ (± .000005). Sr and Pb isotopes were measured using methods described previously [*Kurz and Kammer*, 1991]. During the course of the SWR measurements the average measured value of the NBS 987 standard was .710264 (± .000019, n=18), and the measured values for NBS 981 were $^{206}Pb/^{204}Pb$ = 16.904 ± .016, $^{207}Pb/^{204}Pb$ = 15.450 ± .021, and $^{208}Pb/^{204}Pb$ = 36.568 ± .060 (n=16). Pb isotopic ratios are normalized to the values of *Catanzaro et al.* [1968] for NBS 981. The reproducibility for the standards given above (and used for normalization purposes) are conservative estimates for the two standard-deviation uncertainty of the Sr, Nd, and Pb isotopic measurements given in tables 1-3. The Sr, Nd, and Pb blanks were typically less than 40, 70, and 150 picograms, respectively, and are a negligible contribution to all the measured ratios. All of the isotopic measurements were carried out in the Isotope Geochemistry Facility at Woods Hole Oceanographic Institution.

Helium isotopes were measured on olivine phenocrysts that were hand picked from crushed and sieved 1 to 2 mm size fractions of the lavas. Blanks were roughly 3.5×10^{-11} ccSTP ^4He with atmospheric $^3He/^4He$. Because subaerial lava flows themselves are extensively degassed, the olivines contain the only remnant of magmatic gases. The bulk of the helium within the olivines resides within the melt inclusions [*Kurz*, 1993] and is released by crushing *in vacuo*; all measurements in tables 1-3 were obtained by crushing *in vacuo*. Helium measurements were carried out in olivines, while the Sr, Nd, and Pb were measured on coexisting groundmass. *Garcia et al.* [this volume] have shown that many olivines in the SWR lavas are out of equilibrium with the coexisting basaltic compositions, and that some of them may be xenocrysts. The coherence between the isotopes of Sr, Nd, Pb and He suggests that this

TABLE 1 (continued). Isotopic and Trace Element Data for Historical and Radiocarbon Dated Lava Flows

sample	k7-14	T87-8	k5-05	k7-04	k7-13	k5-28	k7-01	k7-07	k7-08	ha82-05	ks87-02	k5-32
Unit #	8	8	8	9	10	11	12	13	13	14	14	15
age(yrs)	2180	2180	2180	2300	2940	5660	7230	7750	7750	9020	9020	11780
$^{3}He/^{4}He$	8.6	9.2	9.1	8.4	8.3	8.7	9.2	10.1	8.8	13.1	13.1	11.0
±	0.1	0.1	0.2	0.2	0.1	0.2	0.1	0.1	0.1	0.1	0.1	0.2
$^{87}Sr/^{86}Sr$	0.703950	0.703913	0.703936	0.703917		0.703905	0.703830	0.703779	0.703967	0.703821	0.703838	0.703775
$^{206}Pb/^{204}Pb$	18.15	18.10	18.11	18.10	18.19	18.06	18.14	18.10	18.12		18.07	18.09
$^{207}Pb/^{204}Pb$	15.46	15.47	15.47	15.45	15.43	15.46	15.45	15.45	15.46		15.43	15.45
$^{208}Pb/^{204}Pb$	37.93	37.93	37.90	37.85	37.86	37.84	37.84	37.84	37.88		37.82	37.84
$^{143}Nd/^{144}Nd$	0.512814	0.512852	0.51283	0.512853	0.512915	0.512835	0.512878	0.512883	0.51289	0.512864	0.512868	0.512863
MgO			10.04	6.75	16.04	9.45		12.44	7.59	15.59	15.46	7.57
Sr/Y			13.6	13.5	11.5	15.7		13.2	15.6	12.5	12.6	12.7
K/Y			143.5	145.2	119.5	102.5		124.5	138.4	116.0	115.0	131.0
Sr/Nb			31.7	32.4	27.5	35.0		33.8	37.6	34.1	29.9	36.8
K/Sr			10.5	10.8	10.4	6.5		9.4	8.9	9.3	9.1	10.3
Zr/Nb			13.3	13.7	13.2	13.3		14.9	13.2	14.6	13.4	16.7
Zr/Y			5.7	5.7	5.5	6.0		5.8	5.5	5.4	5.7	5.8
K/P			3.2	3.1	2.5	2.8		2.3	1.7	2.9	3.2	3.2
Rb			5.5	6.2	4.1	5.0		3.9	5.6	4.0	4.1	5.2
Sr			301	321	217	308		257	361	242	236	302
Nb			9.5	9.9	7.9	8.8		7.6	9.6	7.1	7.9	8.2
Zr			126	136	104	117		113	127	104	106	137
Y			22.1	23.8	18.9	19.6		19.4	23.1	19.4	18.7	23.7

# Denotes samples for which the trace element data were obtained from a different subsample of the same lava flow.
Most of the Sr, Pb and He measurements from Kurz and Kammer (1991).
*Both radiocarbon and ^{14}C ages are reported relative to calendar year 1950.

TABLE 2: Isotopic and Trace Element Data From Kahuku and Ninole Basalts.

sample	k5-30	k5-11#	k5-23#	k7-34	k7-24	k7-26	k7-27	K7-29	k7-28	K7-19	k7-20
Unit #	16	17	18	19	20	21	22	23	24	25	26
age(yrs)	28150	>31000	>31000	Kealekeku	Kahuku	Kahuku	Kahuku	Kahuku	Kahuku	Ninole	Ninole
$^{3}He/^{4}He$	18.0	14.8	20.0	15.7	16.0	17.4	16.8		15.4		18.5
±	0.4	0.1	0.2	1.0	0.4	0.1	0.2		0.2		0.1
$^{87}Sr/^{86}Sr$	0.703691	0.703689	0.703736	0.703724	0.703678	.703669	.703675	0.70367	0.703692	0.703740	0.703756
$^{206}Pb/^{204}Pb$	18.17	18.17	18.19	18.20	18.13			18.18	18.20	18.19	18.18
$^{207}Pb/^{204}Pb$	15.46	15.45	15.45	15.43	15.43			15.47	15.45	15.44	15.43
$^{208}Pb/^{204}Pb$	37.93	37.91	37.95	37.92	37.84			37.98	37.96	37.94	37.93
$^{143}Nd/^{144}Nd$	0.512831	0.512915	0.512920	0.512925	0.512938	.512927	.512921	0.512934	0.512917		0.512889
MgO(wgt%)		8.70	9.51	19.77	17.96			6.70	19.65	10.40	11.33
Sr/y		12.2		11.7	12.2			10.8	11.1	11.4	12.3
K/Y		117.8		50.7	113.4			109.6		27.8	39.4
Sr/Nb		30.2		31.1	36.1			27.7	28.0	30.0	28.1
K/Sr		9.6		4.3	9.3			10.1		2.4	3.2
Zr/Nb		13.9		13.6	15.4			13.3	13.9	12.9	11.5
Zr/Y		5.6		5.1	5.2			5.2	5.5	4.9	5.0
K/P		2.9		1.4	3.0			2.5		0.9	1.1
Rb (ppm)		5.1	4.3	0.7	3.8			5.4	3.4	0.8	1.4
Sr (ppm)		281	261	190	213			291	199	270	267
Nb (ppm)		9.3		6.1	5.9			10.5	7.1	9.0	9.5
Zr (ppm)		129		83	91			140	99	116	109
Y (ppm)		23.0	22.1	16.2	17.5			26.9	18.0	23.6	21.7

# Denotes samples for which the trace element data were obtained from a different subsample of the same lava flow.
Most of the Sr, Pb and He measurements from Kurz and Kammer (1991).

TABLE 3. Isotopic and Trace Element Data for Submarine South West Rift Lavas

Sample unit #	p5182-1 40	p5-182-4 39	p5-182-6A 38	p5-182-7 37	p5-182-8 36	p5-183-3 35	p5-183-6 34	p5-183-11 32	p5-183-14 31	p5-183-15 30	p5-184-6 33	p5-185-5 29	p5-185-11 28
water depth	1420	1375	1310	1265	1235	1100	1015	790	650	630	1425	1670	1505
depth in section	1250	1205	1140	1095	1065	935	850	625	485	465	785	0-50	0-50
$^{3}He/^{4}He$ (R/Ra)	17.2	18.9	20.0	19.1	16.6	18.7	19.9	13.3	15.9	17.2	18.3	16.9	16.4
±	0.1	0.2	0.3	0.2	0.3	0.3	0.2	0.1	0.1	0.1	0.3	0.2	0.1
^{4}He(ccSTP/g)	6.68E-08	8.21E-09	5.07E-09	9.08E-09	4.01E-09	2.30E-09	1.13E-08	4.16E-08	3.21E-08	1.91E-08	7.34E-09	6.70E-09	1.45E-08
$^{87}Sr/^{86}Sr$	0.703688	0.703676	0.703660	0.703652	0.703682	0.703693	0.703684	0.703623	0.703645	0.703609	0.703682	0.703743	0.703651
$^{206}Pb/^{204}Pb$	18.18	18.25	18.24	18.33	18.25	18.15	18.19	18.23	18.29	18.28	18.19	18.31	18.18
$^{207}Pb/^{204}Pb$	15.46	15.45	15.43	15.52	15.46	15.43	15.43	15.46	15.47	15.45	15.46	15.51	15.47
$^{208}Pb/^{204}Pb$	37.96	37.97	37.94	38.16	38.02	37.89	37.89	38.00	38.03	37.98	37.98	38.21	37.99
$^{143}Nd/^{144}Nd$	0.512932	0.512911	0.512913	0.512928	0.512915	0.512910	0.512911	0.512917	0.512937	0.512928	0.512912	0.512879	0.512880
MgO(wgt %)	21.84	32.28	27.93	32.81	23.28	21.83	11.97	15.13	13.34	17.41	15.78	9.85	9.84
Sr/Y	10.6	11.5	11.8	12.4	11.0	11.4	12.0	12.1	12.1	11.6	11.9	12.2	11.8
K/Y	124.8	125.0	137.2	130.0	122.9	117.9	118.6	118.3	122.1	116.3	134.8	126.1	124.2
Sr/Nb	25.5	22.7	23.9	21.5	23.2	26.7	27.6	28.8	27.8	24.8	28.7	22.8	29.0
K/Sr	11.8	10.9	11.6	10.5	11.1	10.3	9.9	9.8	10.1	10.0	11.3	10.4	10.5
Zr/Nb	13.0	11.1	11.2	9.8	11.2	12.5	12.3	12.7	12.6	11.6	13.1	10.7	13.1
Zr/Y	5.4	5.6	5.6	5.7	5.3	5.3	5.3	5.3	5.5	5.4	5.4	5.7	5.3
Rb (ppm)	4.1	2.3	2.3	2.0	3.5	2.9	4.2	3.9	4.7	4.2	4.5	6.5	4.3
Sr (ppm)	181	102	136	103	172	171	243	216	245	211	221	314	264
Nb (ppm)	7.1	4.5	5.7	4.8	7.4	6.4	8.8	7.5	8.8	8.5	7.7	13.8	9.1
Zr (ppm)	92	50	64	47	83	80	108	95	111	99	101	148	119
Y (ppm)	17.1	8.9	11.5	8.3	15.6	15.0	20.3	17.9	20.2	18.2	18.6	25.8	22.4

is a minor problem, and that even if the olivines are xenocrysts with respect to major elements, the helium within them is closely related to the lavas which carry them.

Trace element data for the Mauna Loa samples, presented in the tables, were measured using X-ray fluorescence (XRF) spectrometry at University of Massachusetts [*Rhodes*, 1983; 1988]. Only key trace element data are presented here; a more complete discussion of major and trace element abundances will be presented elsewhere.

3. RESULTS AND DISCUSSION

3.1. *Temporal Isotopic Evolution of Mauna Loa*

The Sr, Nd, Pb and He isotopic data from tables 1-3 are summarized in Figure 2. Because the exact ages of the Kahuku and Ninole Basalts and the submarine samples are not known, the x axis in this diagram is the stratigraphic order, as represented by the unit number. We emphasize that there are considerable uncertainties in the stratigraphic order, and that use of unit number for plotting purposes does not imply that the age sequence is continuous. As discussed above, without age determinations, it is impossible to evaluate the assumption that the Ninole basalts are older than the Kahuku Basalts, or that there may be overlap between subaerial Kahuku and the submarine SWR samples. The youngest flows are historical or radiocarbon dated, and the ages are given in table 1.

There are coherent temporal variations with respect to all the isotope systems, particularly in the age range near 10 ka (indicated by the dotted line in Figure 2). The $^{3}He/^{4}He$ ratios are highest in lavas older than 10 ka, which are assumed here to relate to the decrease of the hotspot signal at that time. The new Nd isotopic data show that low $^{143}Nd/^{144}Nd$ ratios correlate with high $^{87}Sr/^{86}Sr$, that the oldest samples have the highest Nd isotope ratios, and that Nd also displays an important shift at ~10 ka. However, all the isotopic systems *except helium* display important shifts between the historical and radiocarbon dated flows, which demonstrates that the variations do not simply reflect a simple "shut off" of the hotspot, as would be inferred from the helium isotopes alone.

The isotopic data strongly support the inferred stratigraphy, because the data from the SWR samples extend the isotopic trends found for the ^{14}C dated and Kahuku Basalt. This is illustrated in Figure 3, where the arrows indicate the temporal isotopic evolution [see *Kurz and Kammer*, 1991; *Kurz*, 1993]. The isotopic data for the submarine SWR lavas are consistent with the hypothesis that many of them are older than the Kahuku and Ninole basalts. There is considerable overlap in isotopic compositions, and due to the age uncertainties, it is quite possible that the youngest SWR lavas overlap in age with the oldest Kahuku and Ninole Basalts. However, the Mauna Loa isotopic trends are extremely well defined, suggesting that isotopic measurements are useful as an age constraint. Figure 3 also illustrates that the istotopic compositions of the youngest lavas deviate significantly from the trend found for the SWR and other Kahuku lavas. The "bend" in the Sr-He diagram defined by samples younger than 0.6 ka was previously interpreted to reflect lithospheric influence [*Kurz*, 1993].

Some of the submarine SWR samples differ significantly from the subaerial samples in Pb isotopes, and to a lesser degree in Sr isotopes (Figures 2 and 3). The He and Nd isotopic values are similar to the Kahuku and Ninole Ba-

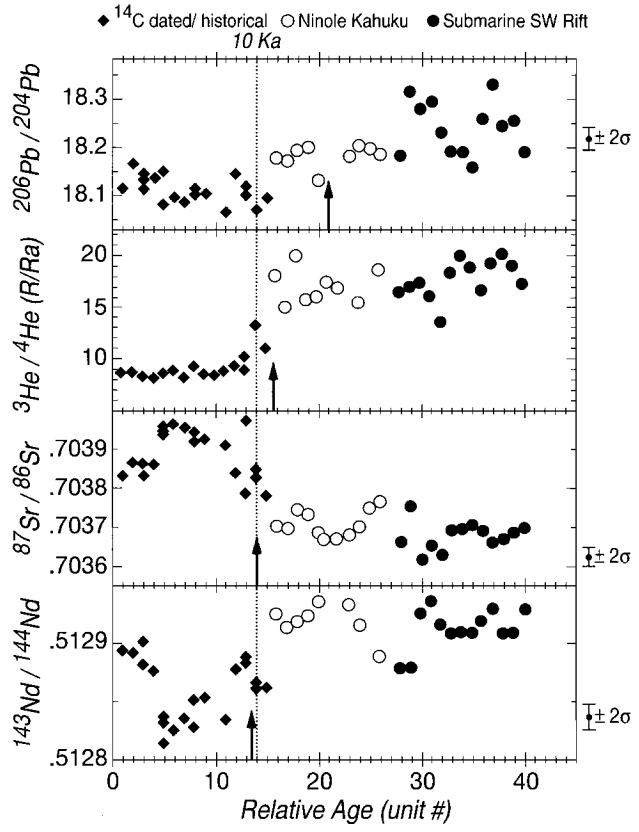

Figure 2. Isotopic composition of Mauna Loa lavas placed in a stratigraphic framework. Numerical ages are known only for those that are less than 30 ka of age (solid diamond symbols, see tables 1 and 2). The x axis is the unit number from tables 1-3, with higher unit numbers having greater age (dotted line indicates 10 ka). The arrows indicate the plume decay half life, which is empirically defined as the age at which the plume isotopic signature has decreased to half its maximum value (or increased in the case of Sr). Note that the oldest lavas have the most radiogenic Pb. The transition at ~10 ka is attributed to diminished influence of the plume.

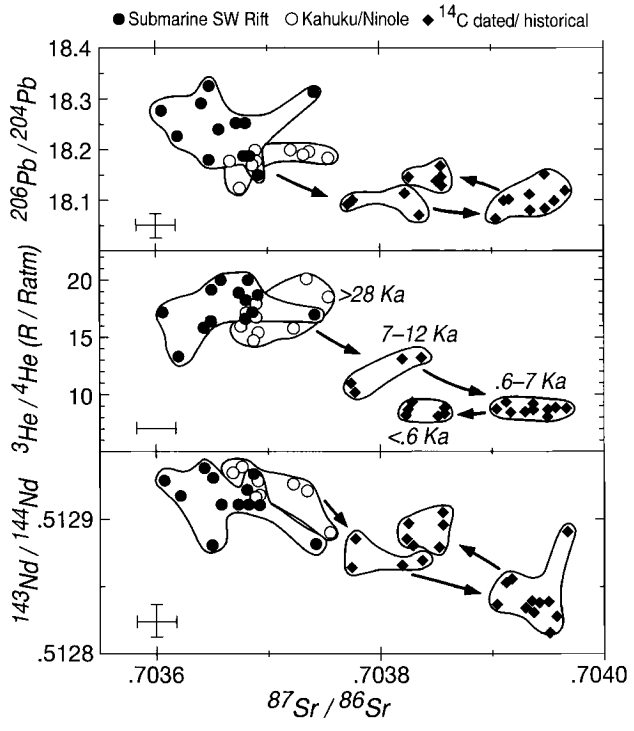

Figure 3. Sr vs. Nd, He, and Pb isotopes for Mauna Loa lavas, with different fields denoting different age ranges (see Figure 2). The complex temporal evolution is indicated by the arrows which indicate time evolution toward the present day. The position of the SWR samples in all of these diagrams is consistent with their age assignment as older than the Kahuku and Ninole samples. Error bars are ± 2σ (error on $^3He/^4He$ is typically smaller than symbols).

salts, but the Pb isotopic ratios found in the SWR samples are the most radiogenic ever reported for Mauna Loa. Assuming that the decrease in $^3He/^4He$ and increase in $^{87}Sr/^{86}Sr$ near 10 ka is due to the shut off of the hotspot, and that the submarine SWR lavas are most representative of the plume isotopic composition, then the Pb isotopic signature of the hotspot disappeared *earlier* than the other isotopic signals. This is illustrated by the arrows in Figure 2, which indicate the time at which the "plume signal" decreased to 1/2 of its maximum (i.e. the unit number which has the value closest to 1/2 the maximum minus the minimum isotopic ratio). The placement of the arrows in Figure 2 highly sensitive to the choice of maximum and minimum values, and there is significant overlap between the SWR and Kahuku lavas. However, assuming that the highest Pb isotopic compositions represent the plume, the Pb isotopes were the first to decrease, followed by He, Sr, and Nd isotopes. For example, at 10 ka (dashed line in Figure 2), the Pb isotopic values are similar to those in younger lava flows, while Sr, Nd, and He differ significantly. The timing derived from this approach is also speculative, due to the lack of geochronology for the older flows. The ages of the Kahuku and Ninole lavas are assumed to be 100 -200 ka [*Lipman et al.*, 1990], and so we can only state that the major shift for Pb isotopes occurred at >100 ka. The major shift in the isotopes therefore occurred at very different times: greater than 100 ka for Pb, at ~14 ka for He, at 9 ka for Sr, and 7.7 ka for Nd.

There are a number of uncertainties in establishing timing differences between the isotopes. First, the hypothesis that the hotspot "shut off" at different times, is based on the assumption that high $^3He/^4He$ ratios are diagnostic of the plume, and that the geochemical transition near 10 ka in the isotopes represents disappearance of the plume component. Figures 2 and 3 show that Sr, Nd and Pb isotopes also varied significantly *after* the "transition", and the assumption that the plume component disappeared

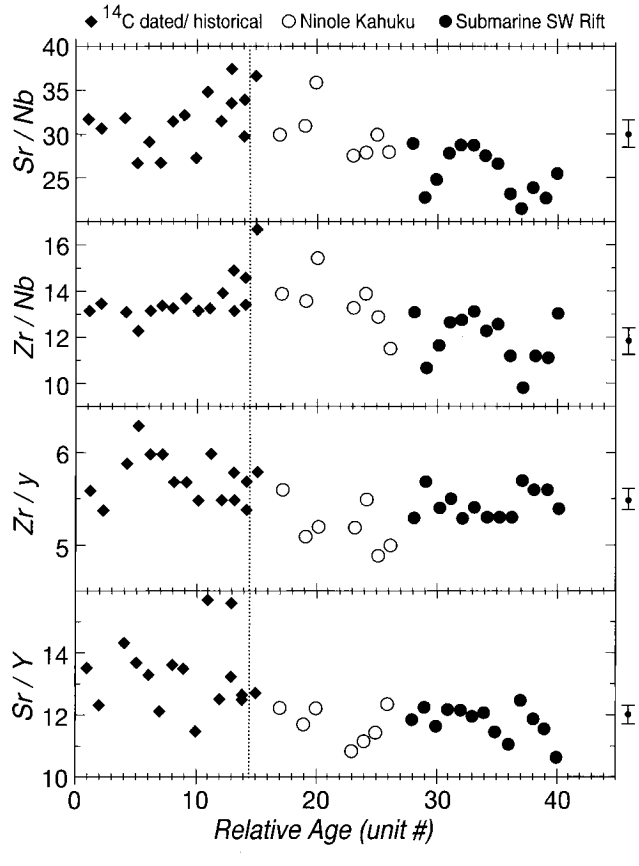

Figure 4. Sr/Nb, Zr/Nb, Zr/Y, and Sr/Y variations as a function of stratigraphic age. Note that both Sr/Nb and Zr/Nb are significantly lower in some of the submarine southwest rift lavas, which are assumed here to be the oldest samples from Mauna Loa. Error bars are ± 2σ.

after 10 ka is based solely on the helium data. With the exception of helium, the isotope and trace element ratios (see below) do not show a monotonic decrease with time. In addition, the Pb isotopes are highly variable within the submarine SWR lavas and do not show a simple stratigraphic decrease. Finally, the timing is based on a relatively sparse data set between approximately 7 and 28 ka.

The apparent timing differences can also be sensitive to the contrast between the plume and the other mantle sources, which relates not just to the differences in isotopic composition, but also to elemental concentrations in the different sources. The total Pb isotopic variation is only 8.5 standard deviations of the measurement uncertainty, and may be more easily affected by concentration differences between the different mantle sources.

3.2. *Temporal Trace Element Variations*

Incompatible trace elements also vary systematically on similar time scales as the isotopes. Figure 4 shows that Zr/Nb and Sr/Nb are lower in some of the SWR lavas than in any of the radiocarbon dated or historical samples. The Kahuku Basalts are transitional between the oldest radiocarbon dated flows and the SWR lavas, and the oldest radiocarbon dated flows have the highest Zr/Nb and Sr/Nb. As with the isotopes, there are also important variations in the younger lava flows, on time scales as short as 100 years [see also *Rhodes and Hart,* this volume]. Ratios involving the more compatible elements such as Zr/Y and Sr/Y (Zr/Y should correlate with Sm/Yb) show less variability in the oldest lavas. Most of the variability within these ratios is found within the youngest lavas, and the radiocarbon dated flows have significantly *higher* Sr/Y and Zr/Y.

The variations with respect to Zr/Nb and Sr/Nb in the older flows are primarily related to Nb concentrations, because there appears to be little temporal variation in the fractionation corrected concentrations of the other elements in the SWR lavas. Figure 5 shows the fractionation normalized (to 7% MgO) concentrations for Sr, Zr, Y, and Nb, based on the assumption that olivine removal and addition are the only controls on the primary trace element concentration [e.g. *Wright,* 1971]. The SWR lavas have higher (MgO normalized) Nb concentrations, while the other elements show little variability in this age range. The youngest lavas, however, have higher fractionation corrected Sr and Zr concentrations.

One possible reason for the differences between the trace elements is that they have differing degrees of incompatibility with respect to silicate/melt partitioning, and are extracted at different rates from the upwelling plume. The

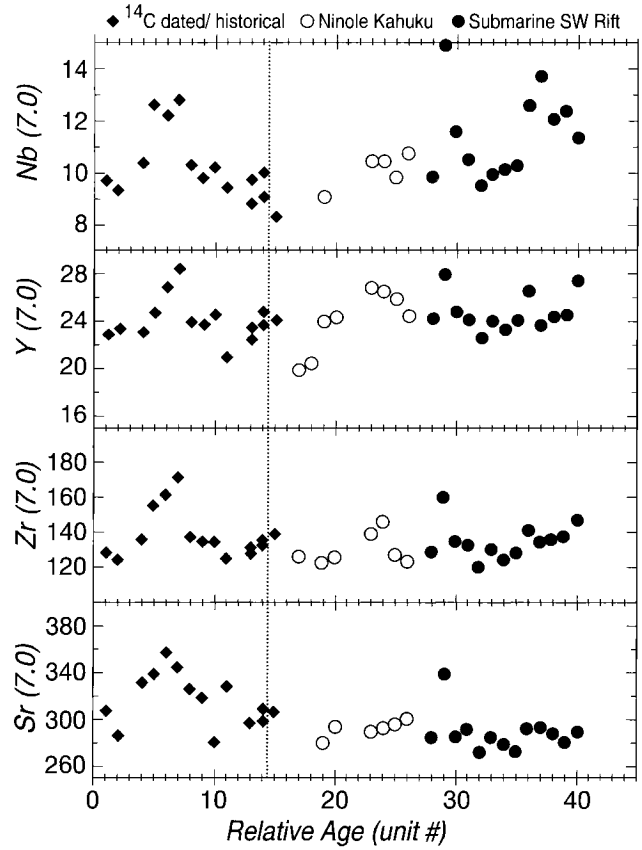

Figure 5. Variations in the fractionation corrected concentrations of Nb, Y, Zr, and Sr as a function of stratigraphic age. The trace elements are normalized to MgO content of 7% for consistency with *Rhodes and Hart* [this volume], although it is possible that the parental magmas are significantly more magnesian than this [*Garcia et al.,* this volume]. The calculations assume that the olivine crystallized have Fo(87), and that they contain no trace elements. Measurement uncertainties are similar in size to the symbols for the elemental abundances.

order of the partition coefficients (Kd) for the elements discussed here should be Nb< Pb < Sr < Nd < Zr < Y, assuming that melting occurs in the garnet stability field [see *Hart and Dunn,* 1993; *Hauri et al.,* 1994]. This order is consistent with Nb (and the isotopic variations), but not with the Zr, Y and Sr data. For example, the Sr/Y and Zr/Y ratios are higher in the youngest lavas, which is the opposite of what would be expected from melting depletion of the plume. The isotopic data suggest different mantle sources for these lavas, and the trace element variations may also be caused by different source concentrations, mixing processes, or variations in melting parameters. Consideration of the Rb/Sr ratios and Sr isotopes suggests mixing of sources or melts plays a role in the variations

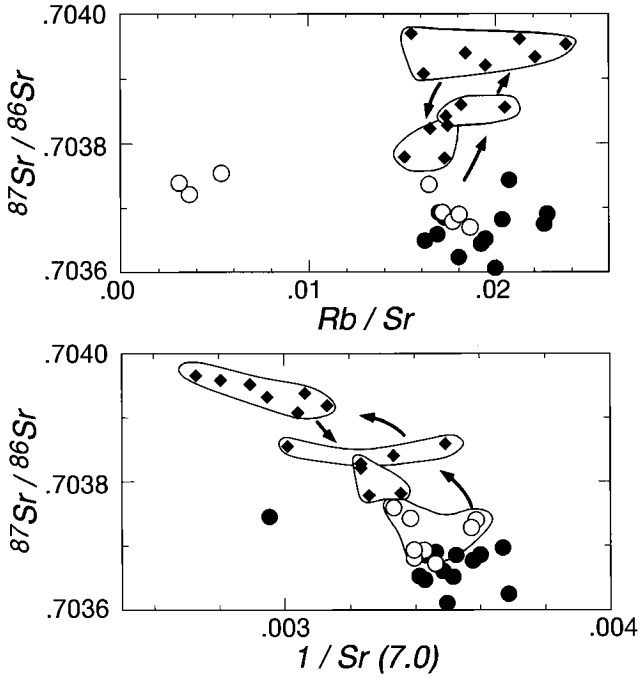

Figure 6. $^{87}Sr/^{86}Sr$ as a function of Rb/Sr and 1/Sr. The lack of a relationship between $^{87}Sr/^{86}Sr$ and Rb/Sr demonstrates that the Rb/Sr ratios in the lavas do not reflect the time integrated source values. The correlation between $^{87}Sr/^{86}Sr$ and 1/Sr suggests that mixing of mantle sources plays a role in the isotopic and trace element variations. Note that higher Sr concentrations are found in the younger lavas (see also Figure 5). Several of the Kahuku lavas have very low Rb/Sr ratios due to Rb loss during subaerial weathering. Arrows denote temporal evolution for the different age groups, as in Figure 3.

(Figure 6). The absence of a relationship between $^{87}Sr/^{86}Sr$ and Rb/Sr demonstrates that the Rb/Sr ratios in the lavas do not reflect the time integrated source values, and must have been altered by mixing and melting processes. The correlation between $^{87}Sr/^{86}Sr$ and 1/Sr supports the hypothesis that mixing of mantle sources or melts plays a role, and shows that higher Sr concentrations characterize the mantle source of the younger lavas. Thus, the high Sr/Y and Zr/Y found in the youngest lavas may reflect higher Sr and Zr concentrations in the source region, which is also consistent with the fractionation corrected Sr and Zr (see Figure 5).

Although the change near 10 ka is referred to here as a "transition", data presented by *Rhodes and Hart* [this volume], and the data from the youngest lavas in Figures 2 and 4 (including some historical flows), provide clear evidence for shorter time scale variations. *Rhodes and Hart* [this volume] found correlations within the historical flows that are distinct from those illustrated by Figure 7, i.e. between $^{87}Sr/^{86}Sr$ and trace element ratios involving the alkalis, such as Sr/Y and K/Y, but *not* with trace element ratios involving Nb. This suggests that the trace element variations in the youngest Mauna Loa flows may be produced by different mechanisms than those governing the variations found in older lavas. Figure 7 shows that there is an overall correlation between Zr/Nb and the isotopes, but that the trend *within* individual age groups is orthogonal to the overall trend. The samples with highest Zr/Nb (the youngest ones) have the highest $^{87}Sr/^{86}Sr$, but the reverse is true within each of the age groups (see for example the Kahuku samples). The distinction between the historical and long term trends is further illustrated by the correlation between $^{87}Sr/^{86}Sr$ and Sr/Y observed for the historical flows [*Rhodes and Hart*, this volume] superimposed on data for the longer time scale presented here (see Figure 8). The data for the older samples, including those from the SWR (see also *Garcia et al.*, [this volume]), dis-

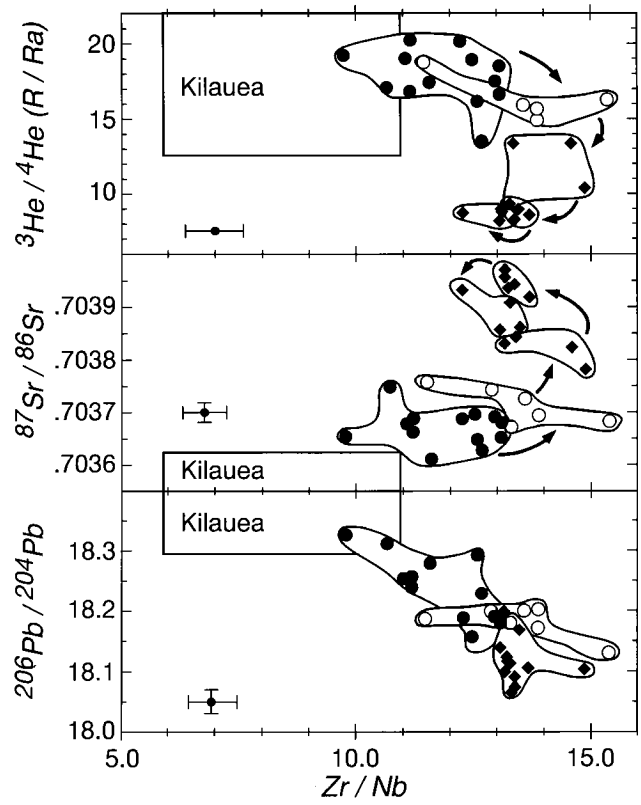

Figure 7. Zr/Nb plotted with respect to the isotopes of Pb, Sr and He for Mauna Loa and Kilauea. The arrows in the top two diagrams denote the temporal evolution, with arrows pointing toward younger ages (as in Figure 3); arrows and distinct fields are omitted from the lower diagram for clarity. Error bars in lower left are $\pm 2\sigma$.

play considerably more scatter, which also probably relates to the different sampling intervals. *Rhodes and Hart* [this volume] attribute the linear trend for the historical data (Figure 8) to mixing between two primary melts. It is possible that the linear historical trend reflects variations in melting parameters (depth and degree of partial melting) primarily reflected in the trace element ratios, while the larger isotopic variability over the longer time scale primarily reflects changes in the mantle source.

In summary, the "transition" in Mauna Loa isotope geochemistry is also found with respect to some trace elements (see Figures 4 and 5). There is considerable scatter in the data, and there are clearly shorter time scale variations, but the Nb concentrations are highest in the submarine SWR lavas. The Nb variations occur with a timing similar to the Pb isotopes, and the transition to low Nb concentrations *precedes* those found for He, Sr, and Nd isotopes. [Despite the scatter within the data from submarine SWR lavas, a two-way t-test suggests that, as a population, they are distinct from the subaerial Kahuku lavas (at the 99% confidence interval) with respect to Nb, Zr/Nb, Sr/Nb, and Pb isotopes.] Therefore, the change in Mauna Loa geochemistry occurs first for Pb isotopes and Nb concentrations, followed by the isotopes of He, Sr, and Nd (in that order). The transition for He, Sr, and Nd occurs at approximately 10 ka; the transition in Pb and Nb occurred at least 100 ka earlier, assuming that the ages of the Kahuku Basalts are between 100 and 200 ka [*Lipman et al.*, 1990]. In contrast to Nb, the concentrations of Sr, Zr, and Y display the largest variability within the youngest lava flows, suggesting that the temporal trace element and isotopic variability is not simply related to degree of incompatibility.

3.3. *Mechanisms for Temporal Variability*

The most reasonable explanation for the large temporal isotopic variations at Mauna Loa, at least those found near 10 ka in age, is that they relate to movement of Mauna Loa over the hotspot. The Pacific plate is moving at an average speed of ~ 10 cm/year, and the typical formation time for Hawaiian volcanoes is between 500 ka and 1 Ma [*Lockwood and Lipman*, 1987; *Moore and Clague*, 1992; *Lipman*, this volume], so it is not unreasonable that Mauna Loa has recently been removed from plume influence. There are many geological arguments suggesting a recent decrease in eruption rates [*Lipman*, this volume] and there is a large change in eruption rates at 10 ka that coincides with the timing of the geochemical variations [*Lockwood*, this volume]. Based on $^{3}He/^{4}He$, the plume influence diminished significantly at ~10 ka. The other data (e.g. Figures 2 and 5) shows that the largest variations in Nb

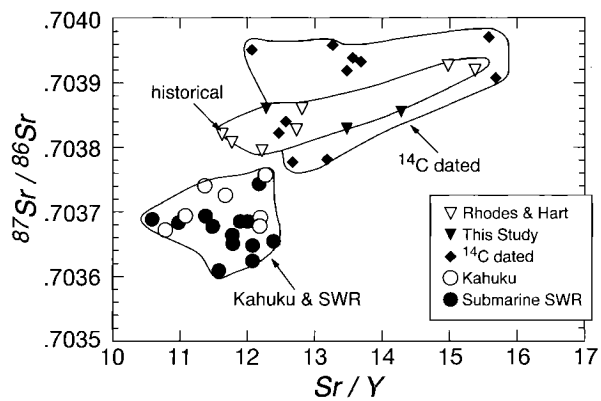

Figure 8. A comparison of Sr/Y and $^{87}Sr/^{86}Sr$ for Mauna Loa lavas. The field for historical encloses both data from table 1 and those of *Rhodes and Hart* [this volume], and shows the distinction between the historical and longer term trends.

concentrations and Pb isotopes are earlier than those for He, Sr and Nd isotopes. There is considerable scatter with respect to Nb concentration and Pb isotopes, but the highest values are found in samples from the submarine SWR. We suggest that the largest variations relate to the decrease in the plume signal indicated by the helium isotopes. The different timing could be partially related to degree of incompatibility, because Nb and Pb are highly incompatible elements. This would suggest a relationship between efficiency of extraction from the upwelling melting column, with the most incompatible elements removed first. The Sr, Y, and Zr concentration data are not consistent with this explanation, because these elements show more variation in the younger lavas (and in the opposite direction expected from melting effects), and no correlation to the isotopic variations in the older lavas. However, the fractionation corrected concentration data are affected by parameters that have lesser affects on the isotope ratios, such as initial concentrations in the different sources, and degree and depth of partial melting. It is possible, for example, to mix two mantle sources having different $^{87}Sr/^{86}Sr$ but very similar Sr concentrations, which could result in an apparent decoupling of the isotope ratio and concentration data.

Os isotopic data provide an important argument that the timing of the isotopic (and Nb) variations are not entirely caused by differing degrees of incompatibility and selective removal by melting. Os is a compatible element with respect to silicate melting, and if incompatibility (and resultant extraction efficiency) were the primary control on the isotopic variations, then Os would be the last isotopic signal to be removed from the plume. However, the Os isotopic data for Mauna Loa show a correlation with Sr, and

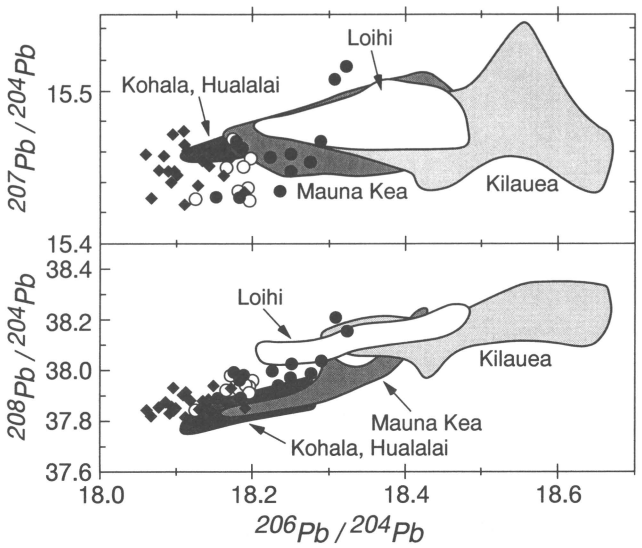

Figure 9. Pb isotopic data for the island of Hawaii. Only data for shield tholeiites are plotted here, in order to allow comparison between the different shields. Data sources: Mauna Loa (this study) Kilauea and Hualalai (unpublished data from this laboratory), Mauna Kea [*Yang et al.*, 1994], Kohala [*Tatsumoto*, 1978], Loihi seamount [*Staudigel et al.*, 1984].

similar temporal variations to those shown in Figure 2 for Sr [*Hauri and Kurz*, 1994; *Hauri et al.*, 1996].

The distinct isotopic and trace element trends observed for the historical flows (Figure 8), as well as the scatter within the submarine SWR lavas strongly suggest that there are several time scales of variability. The 10 to 100 ka variations are attributed to movement of Mauna Loa away from the hotspot. The shorter time scale variations may relate to the geometry of the heterogeneous plume or to the processes of melting and melt migration. The historical lavas have trace element variations that are almost as large as the entire Mauna Loa range, but the isotopic variations are much smaller (see Figure 8), which may imply a greater influence of the melting processes. The variations in Sr/Y may relate to both differing amounts of residual garnet within the source or to variations in Sr/Y within the different sources. Separating the effects of source heterogeneity versus melting parameters will require additional major and trace element data, and is beyond the scope of this paper. *Garcia et al.* [this volume] have shown that glasses from the SWR have similar major element compositions to subaerial Mauna Loa, which would suggest only minor changes in melting parameters over the time period discussed here.

It has been suggested that melt percolation and mixing between two distinct sources could explain the isotopic and trace element variations in Hawaii [*McKenzie and O'Nions*, 1991; *Watson*, 1993]. As mentioned above, although some of the elements show timing variations in order of compatibility (Nb, Pb, He, Sr, Nd), others do not. The Os isotopes present severe problems for percolation models, as discussed above, because Os is a compatible element but correlates with Sr [*Hauri et al.*, 1996]. The two-source melt percolation model also cannot explain the Pb isotopes. This is shown in Figure 9, which illustrates that Loihi seamount lavas are intermediate between Mauna Loa and Kilauea, and therefore cannot represent one of the two end-members, contradicting helium isotopic evidence that Loihi is an end-member. Additionally, any two component mixing in a Pb-Pb diagram will produce a straight line, and percolation cannot produce "loops" (of the kind shown in Figure 3 for the other isotopes) with respect to Pb isotopes. Figure 9 shows that the Mauna Loa data alone do not define a straight line (see the $^{208}Pb/^{204}Pb$ variations). Consideration of the Pb isotopic data for other Hawaiian volcanoes (not shown in Figure 9, such as Haleakala and Koolau) also show significant deviations from a simple mixing line, which excludes a two source mixing model. Additional trace element constraints on melt percolation model have been discussed by *Frey and Rhodes* [1993], and will not be reviewed here. It is sufficient to conclude that a two component melt percolation model of the type discussed by *McKenzie and O'Nions* [1991] cannot explain the temporal evolution of Mauna Loa.

These arguments do not exclude melt migration and solid-melt interaction as important processes within the Hawaiian mantle. Some of the temporal variability on Mauna Loa may be related to degree of incompatibility and hence to melt percolation, the efficacy with which melting removes elements from the plume, and also the extent to which the melts interact with the overlying mantle column. The isotopic data suggest that the temporal variability may also relate to concentration differences between the various sources. It seems most likely that plate motion carries the volcano away from the hotspot source, and that the temporal geochemical variations are produced by a combination of these effects. The largest Pb isotopic variations occur ~100 ka prior to the Sr, Nd, and He decay, and the Pacific plate would have moved only 10 km in this time period, which requires a relatively small scale of mantle heterogeneity.

3.4. *Comparison with Adjacent Volcanoes*

Because the new SWR data extend the known isotopic and trace element range for Mauna Loa, it is important to compare these data with adjacent Hawaiian volcanoes. The trace element and isotope geochemistry of Hawaiian

shield tholeiites has been extensively studied [e.g. *Wright*, 1971; *Tatsumoto*, 1978; *Hofman et al.*, 1984; *Budahn and Schmitt*, 1986; *Tilling et al.*, 1987; *Garcia et al.*, 1989; *Frey and Rhodes*, 1993; *Frey et al.*, 1994; *Leeman et al.*, 1994; *Yang et al.*, 1994], and each shield has apparently distinct geochemical characteristics which may relate to differences in both the mantle source and the physical processes involved. The subaerial lavas of Kilauea and Mauna Loa, the only two presently active volcanoes on the island, are geochemically distinct, even though they are only 30-40 kilometers apart [*Rhodes et al.*, 1989]. However, based on the trace element data presented here, the submarine SWR lavas, which are presumed to be the oldest, are the closest to the values found for Kilauea (see Figure 7). The oldest Mauna Loa samples also have isotopic signatures closest to those of Kilauea, and the age trend suggests a convergence in the geochemistry for older samples. The overlap between the Mauna Loa SWR and Kilauea compositions is supported by the trace element data presented by *Garcia et al.* [this volume], but does not necessarily extend to the major elements. The data presented here illustrate the importance of temporal evolution to comparison between the different shield volcanoes.

Based on the high $^3He/^4He$ found at Loihi seamount, we have proposed that Loihi isotopic data represent the closest approximation to an undegassed plume "end-member" for Hawaii [*Kurz et al.*, 1982; *Kurz et al.*, 1983; *Kurz and Kammer*, 1991; *Kurz*, 1993]. Loihi is also the youngest volcano in the archipelago, suggesting that the high $^3He/^4He$ ratios are related to volcano evolution [*Kurz et al.*, 1983; *Kurz et al.*, 1987]. The new data from SWR of Mauna Loa support this hypothesis because the oldest lavas have the highest $^3He/^4He$ (see Figure 10), and define a trend which is closer to the isotopic composition of Loihi seamount than any of the younger lavas. In addition, all Hawaiian volcanoes have higher $^3He/^4He$ in the oldest tholeiitic lavas than in the associated alkali basalts. At present these generalizations are based on stratigraphic studies at Haleakala, Hualalai, Mauna Kea, Kilauea and Mauna Loa [*Kurz et al.*, 1987; *Kurz and Kammer*, 1991; *Kurz*, 1993; unpublished data this laboratory]. All of these results strongly support the mantle plume model as originally formulated by *Wilson* [1963] and *Morgan* [1971], particularly if high $^3He/^4He$ ratios reflect undegassed mantle sources (i.e. those having high He/(Th+U)) deriving from the lower mantle [e.g. *Kurz et al.*, 1982].

The new data from the SWR of Mauna Loa have a bearing on the relationship between the two parallel chains that form the Hawaiian archipelago. In the islands south east of the Molokai fracture zone, the volcanoes have alternated in time between the two chains, with Loihi,

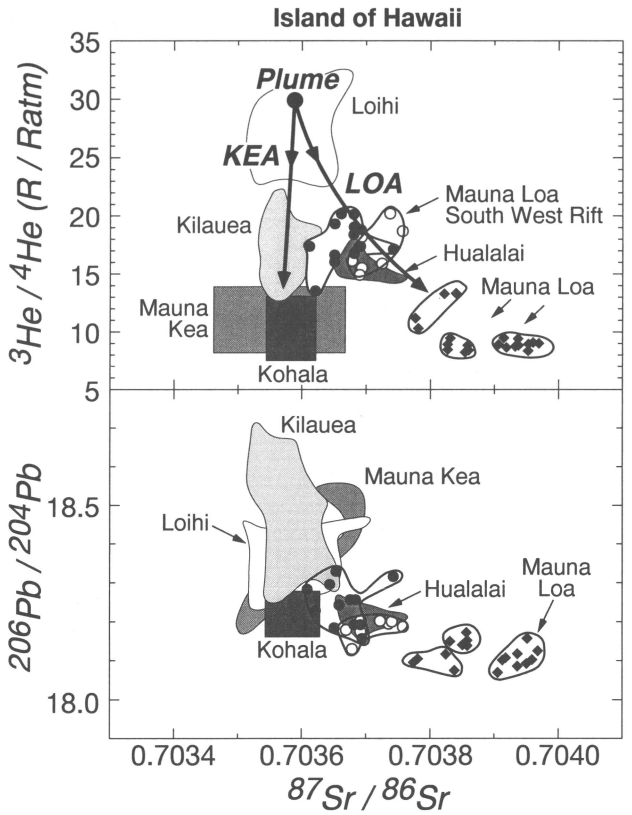

Figure 10. A comparison of the Sr, Pb, and He isotopic compositions for tholeiites on the island of Hawaii. Note that this figure excludes the alkali basalt data for Mauna Kea, Hualalai, and Kohala. Data sources for Loihi seamount: *Kurz et al.*, 1983; *Staudigel et al.*, 1984; Kilauea and Hualalai: unpublished data this laboratory; Mauna Kea: *Kurz et al.*, 1994; Kohala: *Stille et al.*, 1986; *Graham et al.*, 1990]. Although there have been more recent isotopic studies of Loihi seamount [*Garcia et al.*, 1993], the data plotted in this figure (and in Figure 9) are those samples for which helium and other isotopic data coexist for the same samples.

Mauna Loa, Hualalai, Mahukona, Kahoolawe, Lanai and West Molokai representing the southern "Loa" trend, and Kilauea, Mauna Kea, Kohala, Haleakala, West Maui, and East Molokai representing the northern "Kea" trend (e.g., *Jackson et al.*, [1972]; see inset Figure 1). *Tatsumoto* [1978] noticed that the Kea trend volcanoes on the island of Hawaii had more radiogenic Pb isotope ratios, and was the first to relate isotope geochemistry to the existence of the two chains. He suggested that the Loa volcanoes represented the primary expression of the upwelling plume, and that the volcanoes in the Kea trend were more affected by lithospheric contamination (which by inference had high U/Pb) due to lower upwelling and eruption rates and greater interaction with the lithosphere. At present, this

hypothesis remains speculative; no comprehensive explanation has ever been offered for the existence of the two chains, and it is unclear if they are produced by lithospheric loading or mantle processes.

The isotopic data from Mauna Loa support Tatsumoto's suggestion that the Loa and Kea trends are distinguished with respect to isotopic composition on the island of Hawaii (with Kea trend volcanoes having more radiogenic Pb). The new data from the SWR are particularly important because they illustrate that the isotopic and trace element compositions tend to converge for the older shield building tholeiites, and that the geochemical difference between the Loa and Kea trends is primarily a late stage, time dependent effect. The oldest lavas from Kilauea and Mauna Loa are most similar to Loihi, but the last 30 ka of Mauna Loa eruptions have diverged significantly, as reflected in higher $^{87}Sr/^{86}Sr$ and lower $^{3}He/^{4}He$ ratios (see Figure 10). Figure 10 suggests that the Sr and He isotopes can be used to distinguish the Loa and Kea trend volcanoes, with high $^{3}He/^{4}He$ indicative of plume influence. It is unclear how robust this observation is, because there is little data from the other volcanoes in the archipelago that might be used to evaluate it. The Mauna Loa data demonstrate how important the temporal evolution of a single volcano is to such comparisons; it is problematic to compare volcanoes at different stages of their evolution, even though they may be tholeiitic shields.

4. IMPLICATIONS

4.1. *Geochemistry of Hawaiian Basalts*

The temporal variations found at Mauna Loa, particularly with respect to Pb isotopes and Nb concentrations, demonstrate how misleading it can be to compare geochemical data from Hawaiian volcanoes at different stages in their evolution; even within shield building tholeiites, the stratigraphic framework is critical. For example, it is common to consider Koolau as representative of the plume end-member for Hawaiian volcanism, due to the high $^{87}Sr/^{86}Sr$ ratios found in the tholeiites [e.g. *Stille et al.*, 1986; *Leeman et al.*, 1994]. However, the isotopic compositions found at Koolau are similar to the late stage of Mauna Loa , because the high $^{87}Sr/^{86}Sr$ are coupled with unradiogenic Pb isotopes, intermediate $^{3}He/^{4}He$, and low Nb concentrations [*Stille et al.*, 1986; *Roden et al.*, 1994]. The Mauna Loa isotopic and temporal variations, combined with other data from the island of Hawaii, suggest that this set of geochemical characteristics does *not* relate to the plume, but may be a relatively small volume contribution, limited to the last stages of shield building. As discussed below, the "component" represented by isotopic compositions similar to Koolau and late stage Mauna Loa may be explained by entrained asthenosphere or lithosphere. Although this component is clearly associated with the plume and/or its interaction with the lithosphere, the data presented here suggest it is not the most volumetrically important contributor to Hawaiian shields, and probably does not represent the plume itself.

One important implication of the data presented here is that Nb and Pb may be the first elements to be removed from the upwelling plume. This conclusion must be viewed as highly speculative, in light of the isotopic evidence for mixing between different mantle sources, and the possibility that the different timing for changes in Pb and Nb (relative to He, Sr and Nd) is simply caused by concentration differences between the sources. Whether the order of depletion is caused by mixing or melt silicate partitioning, the coherence between helium and the other elements strongly suggests that the physical control on helium isotopes within the melting region is similar to other elements. Therefore, there is little reason to invoke unusual processes, such as vapor phase transfer or metasomatism [e.g. *Vance et al.*, 1990], to "decouple" helium. It seems extremely likely that helium behaves as an incompatible element with respect to melt/silicate partitioning, which is also suggested by phenocryst/glass partitioning [*Kurz*, 1993]. Therefore, the Mauna Loa geochemical data offer little support for models which discard the helium isotopic evidence [e.g. *Hofmann*, 1986].

4.2 *Models for the Hawaiian Plume*

Based on the arguments presented above, it is necessary to reconcile the requirement for three mantle sources, and the temporal geochemical variations, with a reasonable geometry for the upwelling mantle plume beneath Hawaii. Figure 11 shows one highly schematic example of such a model; many other geometries are possible, but this cartoon demonstrates the possibilities with respect to the different geochemical contributions to a Hawaiian volcano [see also *Frey and Rhodes*, 1993]. At least four distinct mantle reservoirs could serve as sources for Hawaiian volcanism: the upwelling plume, entrained material at the edge of the plume, normal asthenospheric mantle, and Pacific plate lithosphere. All of these are possible contributors; although the geochemistry alone cannot conclusively identify them, the isotopic data provide some important constraints.

The highest $^{3}He/^{4}He$ ratios (up to 20 times atmospheric), found in the oldest Mauna Loa flows, identify the mantle plume itself as a major contributor to the main

shield stage. As mentioned above, all known temporal studies of Hawaiian volcanoes show that higher $^3He/^4He$ ratios are found in the earliest shield stages. Normal asthenosphere, and presumably normal lithosphere, have $^3He/^4He$ ratios close to 8 times atmospheric, based primarily on studies of MORB. The lower $^3He/^4He$ ratios in the younger Mauna Loa lavas were originally interpreted as mixing between the plume and entrained mantle at the plume edge [*Kurz and Kammer*, 1991; *Kurz*, 1993]. The geochemical reason for invoking entrained material, as opposed to lithosphere [e.g. *Liu and Chase*, 1991], is that high $^{87}Sr/^{86}Sr$ ratios should not be observed in normal lithosphere, because normal MORB typically have $^{87}Sr/^{86}Sr$ less than .7030 [e.g. *King et al.*, 1993]. However, studies of Hawaiian lherzolite xenoliths, which may represent fragments of the oceanic lithosphere, have $^{87}Sr/^{86}Sr$ of .7035 to .7042 [*Vance et al.*, 1989], making this a relatively weak argument.

Another argument that lithosphere is not extensively involved as a source of melting comes from seismic and modeling studies, which suggest minimal lithospheric thinning beneath Hawaii [*Davies*, 1992; *Ribe and Christensen*, 1994; *Woods et al.*, 1991]. Lithospheric thinning, and the resultant thermal buoyancy, was thought to have produced Hawaiian Swell [*Detrick and Crough*, 1978] which is now in doubt. The new data presented here are important because they demonstrate that the geochemistry of Mauna Loa has changed most dramatically within the last 30 to 100 ka, representing a small fraction of the erupted, and therefore mantle source volume. It is only during the recent eruptions (< 30 ka) that isotopic data indicate a non-hotspot source. The historical Mauna Loa lavas define a "bend" in all of the isotope systems (toward less radiogenic isotopic compositions, see Figure 3), which was previously attributed to the lithospheric component [*Kurz*, 1993].

The model shown in Figure 11 assumes that the geochemical variations are related to heterogeneity within the plume rather than lithospheric involvement, due to the seismic observations, the relatively radiogenic Sr isotopic compositions in recent Mauna Loa, as well as the Os isotopic evidence [*Hauri et al.*, 1996].

The order of element removal suggested by Figure 2 is consistent with the cartoon in Figure 11, if we assume that the end of shield building stage represents a fundamental change in the mantle source. The model presumes that all melting occurs within the garnet stability field (depths greater than 90 Km), and attributes the geochemical change between 10 and 100 ka to zonation within the plume. At the end of shield building, the melting rate decreases and the geochemical signature of the plume diminishes. It is at this stage that the geochemical signature of the entrained material, which accumulates at the base of the lithosphere, may become dominant. It is possible that this component has been melting all along, but has been overwhelmed by melts from the closely associated, and volumetrically more important, plume material. The different timing implied by Figure 2 could then be explained by the concentration differences within the heterogeneous plume, combined with differing degrees of incompatibility (i.e. Pb and Nb having greatest concentration most effectively partitioned into the melt).

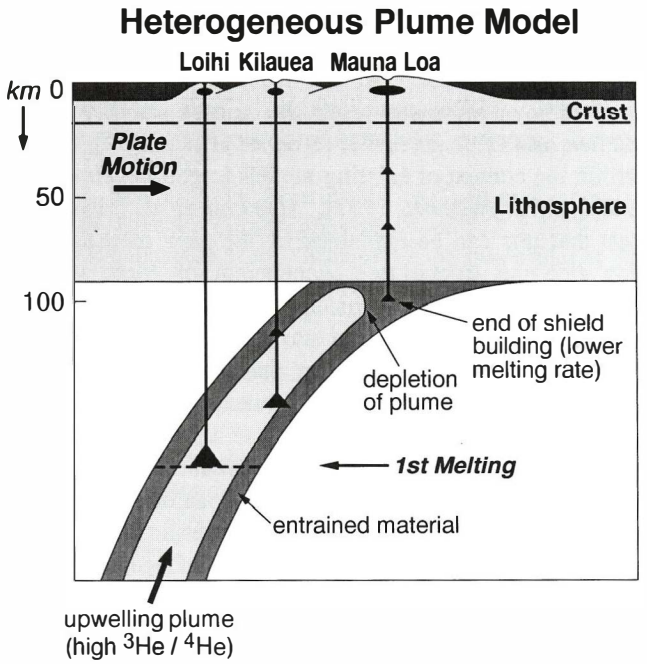

Figure 11. One highly schematic model for the Hawaiian plume, which could explain the temporal geochemical variations. The model illustrates that there are several possible mantle sources, including a heterogeneous plume, the surrounding asthenosphere, and the lithosphere. Melting begins in the garnet stability field. By the time shield building is complete, the plume isotopic signature may have been partly removed due to extensive melting of the plume, and the plume is assumed to be concentrically zoned. The last stage of shield building, as represented by recent Mauna Loa lavas, has contributions from entrained mantle material. It is inferred that the melting rate decreases at the end of shield building, which could imply slower melt migration rates through the lithosphere. Lithospheric involvement is assumed to be minimal, and limited to post-shield lavas. The absence of a depth scale below 100 km is intentional and is intended to emphasize the uncertainty in the depth for initiation of melting.

There is considerable evidence that melting beneath Hawaii occurs within the garnet stability field [*Budahn and Schmitt*, 1985; *Frey and Rhodes*, 1993; *Wright*, 1971;

Hofman et al., 1984; *Salters and Hart*, 1991]. In addition, the lack of Th-U disequilibrium within the historical tholeiites of Mauna Loa and Kilauea suggest relatively slow removal of melts from the garnet stability region [*Cohen and O'Nions*, 1993; *Hemond et al.*, 1994], at least within the context of existing models [e.g. *Spiegelman and Elliot*, 1993; *Iwamori*, 1993]. *Hemond et al.* [1994] suggest that this can be explained by the slow melt aggregation (via the fractal tree mechanism of *Hart*, [1993]), followed by rapid transit through the lithosphere. Identification of the mechanics, and site of, the mantle/melt interaction are critical to evaluating the use of mantle mixing schemes [e.g., *Hart et al.*, 1992], to explain global isotopic variations.

One serious problem with the model shown in Figure 11 is that it is not entirely consistent with major element data. Variations in depth of melting should result in systematic major element variations as a function of age. Although each volcano on the island of Hawaii has distinct major element chemistry [e.g. *Frey and Rhodes*, 1993], Mauna Loa does not show temporal major element variations on the time scale discussed here [*Garcia et al.*, this volume]. Further evaluation must await consideration of a more comprehensive major element data set.

Finally, the new data from Mauna Loa, and the general convergence toward the isotopic characteristics of Loihi seamount for the oldest Hawaiian shield tholeiites (see Figure 10), support the hypothesis that Loihi seamount represents the present day expression of the plume center. The hypothesis that Mauna Loa has been removed from the hotspot within the last 10 ka would require the radius of the plume to be less than 40 kilometers (the distance between Mauna Loa and Loihi). This is consistent with the simple calculation of plume radius from the shield building time of 500 ka, combined with plate motion of 10 cm/year, which yields 50 Km. Although the reason for the Loa and Kea trends remains enigmatic, the Mauna Loa data suggest that isotopes can be used to distinguish them (particularly Sr and He) and that these geochemical differences relate to the end of shield building.

5. CONCLUSIONS

1. The new He, Sr, Nd, and Pb isotopic data for the submarine SWR reported here extend the known range of isotopic values for Mauna Loa, particularly for Pb isotopes. The fact that these data continue the temporal trends found for subaerial (stratigraphically placed and ^{14}C dated) lava flows, strongly suggests that the SWR lava flows are older than the Kahuku and Ninole basalts. The coherence of the isotopic data also demonstrates that helium is removed from the mantle by melting processes rather than metasomatic processes or vapor transfer, and is not affected by magma chamber contamination processes.

2. He, Sr, and Nd isotopic compositions in the submarine SWR lavas are similar to the Kahuku and Ninole Basalts, but Pb is significantly more radiogenic, suggesting that the Pb isotopic signature of the mantle plume decreased significantly earlier. The new data from the SWR lavas, combined with existing isotopic data from subaerial Mauna Loa, suggest that the order of removal of the plume isotopic signature is Pb (>100 ka), He (~14 ka), Sr (9 ka), and Nd (8 ka), which may relate to the order of silicate/melt partitioning and to concentration differences in the different mantle sources. Zr/Nb and Sr/Nb, and fractionation corrected Nb concentrations, correlate with the isotopes, and also show significant variations on the 100 ka time scale. The assignment of different timing for the different isotopes, particularly Sr, Nd, and He, must be viewed as speculative due to the limitations of the data set, but is a testable hypothesis, given the large number of Mauna Loa lava flows of known age [*Lockwood*, this volume].

3. Superimposed on the 10 to 100 ka temporal variations, there are also important shorter term variations, as demonstrated by the scatter within the submarine SWR samples, and data from historical samples [*Rhodes and Hart*, this volume]. The isotopic and trace element trends are distinct for the historical lavas, suggesting that different processes are responsible for the variability on the two different time scales. The historical variations (e.g. Figure 8) may be related to melting effects, while the longer term trend can be attributed to removal of the plume source from Mauna Loa.

4. The temporal isotopic evolution of Mauna Loa suggests that the Loa and Kea volcanoes can be distinguished based on isotopes, particularly He, Sr, and Pb, but that the differences are primarily found in the last stages of shield building. The model suggested here (Figure 11) relates the geochemical differences to a heterogeneous, zoned plume, and the changing dynamics of melting within the plume at the end of shield building (as it impinges on the lithosphere). The temporal isotopic evolution of Mauna Loa also supports the hypothesis that Loihi seamount isotopic compositions best represent the plume end member for Hawaiian volcanoes.

Acknowledgments. This work was supported by NSF OCE92-14006 and EAR93-18889 to MK and OCE90-12030 to MG. We thank the Pisces V diving team, led by Terry Kerby, for their assistance in sample collection, and Peter Lipman and Tom Hulsebosch for assistance with the dive program and numerous

discussions. Constructive reviews by Fred Frey, Peter Lipman, and Gene Yogodzinski greatly improved the manuscript. MK gratefully acknowledges the encouragement of J. Lockwood and F. Truesdell at HVO, and the field mapping effort at HVO which has made detailed study of Mauna Loa possible. This is WHOI contribution number 9038, and SOEST contribution number 3940.

REFERENCES

Budahn, J.R. and R.A. Schmitt, Petrogenetic modeling of Hawaiian tholeiitic basalts: a geochemical approach. *Geochim. Cosmochim. Acta 49*, 67-87, 1986.

Catanzaro, E.J., T.J. Murphy, W.R. Shields, and E. Garner, Absolute isotopic abundance ratios of common, equal atom and radiogenic lead isotope standards. *J. Res. NBS. 72A*, 261, 1968.

Cohen, A.S., and R.K. O'Nions, Melting rates beneath Hawaii: evidence from uranium series isotopes in recent lavas. *Earth Planet. Sci. Lett. 120*, 169-175, 1993.

Condomines, M., K. Gronvold, P.J. Hooker, K. Muehlenbachs, R.K. O'Nions, J. Oskarsson, and E.R. Oxburgh, Helium, oxygen, strontium and neodymium relationships in Icelandic volcanics. *Earth Planet. Sci. Lett. 66*, 125-136, 1983.

Davies, G.F., Temporal variation of the Hawaiian plume flux. *Earth and Planetary Science Letters 113*, 277-286, 1992.

Detrick, R.S., and S. T. Crough, Island subsidence, hot spots and lithospheric thinning. *J. Geophys. Res. 83*, 1236-1244, 1978.

Fornari, Peterson, Lockwood, Malahoff, and Heezen, Submarine extension of the SWRZ of Mauna Loa volcano, Hawaii. *GSA Bull. 90*, 435-443, 1979.

Frey, F.A. and J.M. Rhodes, Intershield geochemical differences among Hawaiian volcanoes: implications for source compositions, melting process and magma ascent paths. *Phil. Trans. Roy. Soc. London A342*, 121-136, 1993.

Frey, F.A., M.O. Garcia, and M.F. Roden, Geochemical characteristics of Koolau volcano: implications of intershield geochemical differences among Hawaiian volcanoes. *Geochim. Cosmochim. Acta 58*, 1441-1462, 1994

Garcia, M.O, D. Muenow, K. Aggrey, and J. O'Neil, Major element, volatile and stable isotope geochemistry of Hawaiian submarine tholeiitic glasses. *J. Geophys. Res. 94*, 10525-10538, 1989.

Garcia, M.O., T.P. Hulsebosch, and J. M. Rhodes, Glass and Mineral Chemistry of Olivine-Rich submarine basalts, South West Rift Zone, Mauna Loa Volcano: Implications for magmatic processes, this volume.

Garcia, M.O., J.J. Mahoney, and E. Ito, An evaluation of temporal geochemical evolution Loihi summit lavas: results from Alvin submersible dives. *J. Geophys. Res. 98*, 537-550, 1993.

Graham, D., J. Lupton, M. Garcia, He isotopes in olivine phenocrysts from submarine basalts of Mauna Kea and Kohala, Island of Hawaii. *EOS (Trans. AGU) 71*, 657, 1990.

Hart, S.R., Equilibration during mantle melting: A fractal tree model. *Proc. National Acad. Sci. U.S.A. 90*, 11914-11918, 1993.

Hart, S.R., E.H. Hauri, L.A. Oschmann and J.A. Whitehead, Mantle plumes and entrainment: Isotopic evidence. *Science 256*, 517-520, 1992.

Hart, S.R., and T. Dunn, Experimental cpx/melt partitioning of 24 trace elements. *Contrib. Mineral. Petrol. 113*, 1-8, 1993.

Hauri, E.H., and M.D. Kurz, Osmium isotope systematics of the Hawaiian hotspot: contrasting time-series results from Kilauea and Mauna Loa. *EOS (trans. Am. Geophys. Union) 75*, 708, 1994.

Hauri, E.H., J.C. Lassiter, D.J. DePaolo, and J.M. Rhodes, Osmium isotope systematics of drilled lavas from Mauna Loa, Hawaii. *J. Geophys. Res. (submitted)*, 1996.

Hauri, E.H., T.P. Wagner, and T.L. Grove, Experimental and natural partitioning of Th, U, Pb and other trace elements between garnet, clinopyroxene and basaltic melts. *Chem. Geol.* 117-166, 1994.

Hemond, C., A.W. Hofmann, G. Heusser, M. Condomines, I. Raczek, J.M. Rhodes, U-Th-Ra systematics in Kilauea and Mauna Loa basalts, Hawaii. *Chem. Geol. 116*, 163-180, 1994.

Hilton, D. R., J. Barling, and G.E. Wheller, Effect of shallow level contamination on the helium isotope systematics of ocean island lavas. *Nature 373*, 330-333, 1995.

Hofmann, A.W., Nb in Hawaiian magmas: constraints on source composition and evolution. *Chem. Geol. 57*, 17-30, 1986.

Hofmann, A.W., M.D. Feigenson, and I. Raczek , Case studies on the origin of basalt: Petrogenesis of the Mauna Ulu eruption, Kilauea, 1969-1971, *Contrib. Mineral. Petrol. 88*, 24-35, 1984.

Hofmann, A.W., K.P. Jochum, M. Seufert, and W.M. White, Nb and Pb in oceanic basalts: New constraints on mantle evolution. *Earth Planet. Sci. Lett. 79*, 33-45, 1986.

Iwamori, H., Dynamic disequilibrium melting model with porous flow and diffusion controlled chemical equilibration. *Earth Planet. Sci. Lett 114*, 301-313, 1993.

Jackson, E.D., E.A. Silver, and G.B. Dalrymple, Hawaiian-Emperor Chain and its relation to Cenozoic circumpacific tectonics. *Bull. Geol. Soc. Am. 83*, 601-618. 1972.

King, A. J., D G. Waggoner, and M. O. Garcia, "Geochemistry and petrology of basalts from leg 136, central Pacific Ocean", in: R. H. Wilkens, J. Firth, J. Bender, et al, (1993) *Proceedings of the Ocean Drilling Program, Scientific Results*, Vol. 136: College Station, TX (Ocean Drilling Program), 1993.

Kurz, M. D., Mantle heterogeneity beneath oceanic islands: some inferences from isotopes. *Proceedings of the Royal Society of London A342*, 91–103, 1993.

Kurz, M.D., W.J. Jenkins, and S.R. Hart, Helium isotopic systematics of oceanic islands: implications for mantle heterogeneity. *Nature 297*, 43-47, 1982.

Kurz, M.D., W.J. Jenkins, S. Hart, and D. Clague, Helium isotopic variations in Loihi Seamount and the island of Hawaii. *Earth Planet. Sci. Lett. 66*, 388-406, 1983.

Kurz, M.D., M.O. Garcia, F.A. Frey and P.A. O'Brien, Temporal helium isotopic variations within Hawaiian volcanoes: basalts

from Mauna Loa and Haleakala. *Geochim. Cosmochim. Acta 51*, 2905-2914, 1987.

Kurz, M.D., and D.P. Kammer, Isotopic evolution of Mauna Loa Volcano. *Earth Planet. Sci. Lett. 103*, 257-269, 1991.

Kurz, M.D., J.K. Lassiter, B.M. Kennedy, D.J. DePaolo, J.M. Rhodes, and F. A. Frey, Helium isotopic evolution of Mauna Kea volcano:first results from the 1 km drill core. *EOS (Trans. Am. Geophys. Union) 75*, 711, 1994.

Leeman, W.P., D.C. Gerlach, M.O. Garcia, and H.B. West, Gecohemical variations in lavas from Kahoolawe volcano, Hawaii: evidence for open system evolution of plume-derived magmas. *Contrib. Mineral. Petrol. 116*, 62-77, 1994.

Lipman, P.W., Growth of Mauna Loa volcano during the last hundred thousand years: rates of lava accumulation versus gravitational subsidence, this volume.

Lipman, P.W., and A. Swenson, Generalized geological map of the southwest rift of Mauna Loa, U.S. Geol. Surv. Map I-1323, 1984.

Lipman, P.W., J.M. Rhodes, and G.B. Dalrymple, The Ninole Basalt-implications for the structural evolution of Mauna Loa volcano, Hawaii. *Bull. Volcanol. 53*, 1-19, 1990.

Liu M. and C.G. Chase, Evolution of Hawaiian basalts: a hotspot melting model. *Earth Planet. Sci. Lett. 104*, 151-165, 1991.

Lockwood, J.P., Mauna Loa Eruptive History-the radiocarbon record, this volume.

Lockwood, J.P., and P.W. Lipman, Holocene eruptive history of Mauna Loa volcano. *U.S. Geological Survey Professional Paper 1350*, 509-536, 1987.

McKenzie, D. and R.K. O'Nions, Partial melt distributions from inversion of rare earth element concentrations. *J. Petrol. 32*, 1021-1091, 1991.

Moore, J.G., Subsidence of the Hawaiian Ridge. *U.S. Geological Survey Professional Paper 1350*, 85-100, 1987.

Moore, J.G., W.R. Normark, and B.J. Szabo, Reef growth and volcanism on the submarine southwest rift zone of Mauna Loa. *Bull. Volcanol. 52*, 375-380, 1990.

Moore, J.G., and D.A. Clague, Volcano growth and evolution of the island of Hawaii. *Bulletin of the Geological Society of America 104*, 1471-1484, 1992.

Morgan,W.J., Convection plumes in the lower mantle. *Nature 230*, 42-43, 1971.

Rhodes, J.M., Homogeneity of lava flows: chemical data for historical Mauna Loa eruptions. *J. Geophys. Res. Supp. 88*, A869-A879, 1983.

Rhodes, J.M., Geochemistry of the 1984 Mauna Loa eruption: implications for magma storage and supply. *J. Geophys. Res. 93*, 4453-4456, 1988.

Rhodes, J.M., K.P. Wenz, C.A. Neal, J.W. Sparks, and J.P. Lockwood, Geochemical evidence for invasion of Kilauea's plumbing system by Mauna Loa magma. *Nature 3376*, 257, 1989.

Rhodes, J.M., and S.R. Hart, Episodic trace element and isotopic variations in historic Mauna Loa lavas: implications for magma and plume dynamics, this volume.

Ribe, N.M, and U.R. Christensen, Three dimensional modeling of plume-ltihosphere interaction. *Journal Geophysical Research 99*, 669-682, 1994.

Roden, M.F., T. Trull, S.R. Hart, F.A. Frey, New He, Nd, Pb and Sr isotopic constraints on the constitution of the Hawaiian plume: Results from Koolau Volcano, Oahu, Hawaii, USA. *Geochim. Cosmochim. Acta. 58*, 1431-1440, 1994.

Rubin, M., L.K. Gargulinski, and J.P. McGeehin, Hawaiian radiocarbon dates. *U.S. Geological Survey Prof. Paper 1350*, 213-242, 1987.

Salters, V.J.M, and S.R. Hart, The mantle sources of ocean ridges, islands and arcs: the Hf-isotope connection. *Earth Planet. Sci. Lett. 104*, 364-380, 1991.

Spiegelman, M., and T. Elliot, Consequences of melt transport for uranium series disequilibrium in young lavas. *Earth Planet. Sci. Lett. 118*, 1-20, 1993.

Staudigel H., A. Zindler, S.R. Hart, T. Leslie, C.Y. Chen, and D. Clague, The isotope systematics of a juvenile volcano: Pb, Nd, and Sr isotope ratios of basalts from Loihi Seamount. *Earth Planet. Sci. Lett. 69*, 13-29, 1984.

Stille, P., D.M. Unruh, and M. Tatsumoto, Pb, Sr, Nd, and Hf isotopic constraints on the originof Hawaiian basalts and evidence for a unique mantle source. *Geochim. Cosmochim. Acta 50*, 2303-2319, 1986.

Tatsumoto, M., Isotopic composition of lead in oceanic basalt and its implication to mantle evolution. *Earth Planet. Sci. Lett. 38*, 63-87, 1978.

Tilling, R.I., T.L. Wright, and H.P Millard, Trace element chemistry of Kilauea and Mauna Loa is space and time: a reconnaissance. *U.S.G.S. Prof. Paper 1350*, 641-689, 1987.

Vance D., J.O.H. Stone, and R.K. O'Nions, He, Sr, and Nd isotopes in xenoliths from Hawaii and other oceanic islands. *Earth Planet. Sci. Lett. 96*, 147-160, 1989.

Watson, S. , Rare earth element inversions and percolation models for Hawaii. *Journal of Petrol. 34*, 763-783, 1993.

Wilson, J.T., A possible origin of the Hawaiian Islands. *Can. J. Phys. 41*, 863-870, 1963.

Woods, M.T., J.J. Leveque, and E.A. Okal, Two station measurements of Rayleigh wave group velocity along the Hawaiian swell. *Geophys. Res. Lett. 18*, 105-108, 1991.

Wright, T.L., Chemistry of Kilauea and Mauna Loa in space and time. *U.S. Geological Survey Professional Paper 735*, 1-49, 1971.

Yang, H, F.A. Frey, M.O. Garcia, D.A. Clague, Submarine lavs from Mauna Kea volcano, Hawaii: implications for Hawaiian shield stage processes. *J. Geophysical Research 99*, 15,577-15594, 1994.

Zindler, A. and S.R. Hart, Helium: Problematic primordial signals. *Earth Planet. Sci. Lett. 79*, 1-8, 1986.

M. D Kurz, T. C Kenna, D. P. Kammer, Department of Marine Chemistry and Geochemistry, MS 25, Woods Hole Oceanographic Institution, Woods Hole, MA 02543-1541.

J. Michael Rhodes, Department of Geology and Geography, University of Massachusetts, Amherst, MA 01003.

Michael O. Garcia, Hawaii Center for Volcanology, Geology and Geophysics Department, University of Hawaii, Honolulu, HI 96822.